AAS 19-632

IMPLEMENTATION RECOMMENDATIONS AND USAGE BOUNDARIES FOR THE TWO-DIMENSIONAL PROBABILITY OF COLLISION CALCULATION

Doyle T. Hall*

The two-dimensional (2D) probability of collision (P_c) estimation method relies on several assumptions that must be satisfied for accurate results. Monte Carlo analysis of ~44,000 conjunctions indicates that 2D-P_c provides accurate estimates for most typical conjunctions, but occasionally underestimates P_c significantly, indicating an assumption violation. A test to detect large-amplitude underestimation inaccuracies can be based on how much "offset-from-TCA" 2D-P_c values vary during a well-defined time interval bracketing closest approach. The test successfully detects all large-amplitude 2D-P_c underestimations found to date, but with a high false-alarm rate. The analysis also provides implementation recommendations and usage boundaries for the 2D-P_c method.

INTRODUCTION

The two-dimensional probability of collision approximation, which first entered the literature in 1992[1] and is used by many conjunction assessment practitioners, relies on several assumptions that must be satisfied in order to produce accurate results.[2,3] High-fidelity brute force Monte Carlo (BFMC) simulations, which do not invoke these assumptions, can be used to test the accuracy of the 2D-P_c method.[4] BFMC analysis of ~44,000 conjunctions indicates that the 2D-P_c approximation provides sufficiently accurate estimates to enable effective collision risk assessment for the vast majority of events processed by NASA's Conjunction Assessment Risk Analysis (CARA) team. This majority generally corresponds to high relative-velocity encounters between well-tracked objects. However, for about 0.05% of the analyzed conjunctions, 2D-P_c underestimates the BFMC-P_c value by a factor of 2.5 or more. In several cases, the 2D-P_c method underestimates by a factor of 10 or more. This study focuses on developing a test to detect such large-amplitude 2D-P_c underestimation inaccuracies.

THE 2D-P_c COLLISION PROBABILITY ESTIMATION METHOD

In 1992, Foster and Estes[1] originally developed the 2D-P_c method to quantify collision risks posed to the International Space Station by other cataloged Earth-orbiting satellites. The method approximates P_c values semi-analytically using 2-dimensional (2D) numerical integration. In 2000, Akella and Alfriend[2] reformulated the theory to show how a 2D-P_c estimate can be equivalently expressed as a time integral spanning the entire duration of an on-orbit encounter.[4] A conjunction's 2D-P_c

*Senior Conjunction Assessment Research Scientist, Omitron Inc., 555 E. Pikes Peak Ave, #205, Colorado Springs, CO 80903.

estimate depends on the combined hard-body radii of the primary and secondary satellites involved in the encounter, as well as their mean orbital trajectories and associated position uncertainties.[1-3,5] As discussed in detail by Chan[3] and Coppola[5], the 2D-P_c method also relies on several assumptions that must be sufficiently satisfied in order to provide accurate P_c estimates.

2D-P_c Estimation Method Assumptions

Three important assumptions[1-3,5] underlie the 2D-P_c formulation:

1) At the conjunction's nominal time of closest approach (TCA), the relative primary-to-secondary position uncertainty distribution can be approximated as a single Gaussian — i.e., a multivariate normal distribution calculated using a single 3×3 covariance matrix.

2) During the event, the relative satellite trajectories can be approximated as rectilinear.

3) During the event, the relative position covariance matrix can be approximated as unchanging, or constant in time.

If any of these three assumptions are violated, then 2D-P_c estimates can be inaccurate. Assumption 1 relies on both objects having high quality, recent tracking data and orbital determination (OD) solutions[6,7] for which the relative position covariance provides an accurate approximation of the actual uncertainty. The existence of a non-positive definite (NPD) state covariance matrix[8] provides one example of a violation of assumption 1. The linear-encounter assumption 2 and constant-covariance assumption 3 both rely on the event being a "short-encounter" interaction[5], which is naturally satisfied for high relative-velocity events, but not necessarily for slower interactions such as encounters between closely-spaced, nearly co-orbiting objects.

Short-Term Encounter Validity Interval

As mentioned previously, Akella and Alfriend[2] show that a 2D-P_c estimate can be expressed using a time integral, indicating that collision probability accumulates over a finite period of time during an encounter between two tracked objects — which can also be demonstrated using Monte Carlo methods.[4] A conjunction's effective duration can be considered to be the period in which P_c increases from zero up to a final value to within some precision tolerance level (corresponding to ~10^{-16} for double-precision numerical processing).[3,5] In addition, Chan's analysis[3] of 2D-P_c validity requirements indicates that the linear-encounter assumption must be satisfied throughout an encounter region spanning 17 relative position uncertainty standard deviations (i.e., within ±8.5σ of the point of closest approach). Coppola's analysis[5] extends this concept even further, indicating that both the linear-encounter and constant-covariance assumptions must be satisfied throughout a well-defined time span, TCA ± Δ*t*, known as the *short-term encounter validity interval*, which has half width

$$\Delta t = \max(|\tau_0|, |\tau_1|, \tau_1 - \tau_0) \tag{1}$$

Here τ_0 and τ_1 denote the beginning and ending of the conjunction duration,[5] measured relative to TCA, which depend on the precision tolerance (taken to be $\gamma = 10^{-16}$ for all analyses presented here), as well as the TCA primary-to-secondary relative position vector and associated covariance matrix. (Coppola[5] provides detailed expressions for τ_0 and τ_1 that are not reproduced here.) Short-term encounter validity intervals vary from conjunction to conjunction, with high relative-velocity events having shorter Δt values than slower interactions.

Offset-from-TCA 2D-P_c Estimate Variations

Normally, 2D-P_c estimates employ relative positions and covariances estimated precisely at a conjunction's nominal TCA — the time when the distance between the best-estimate (mean) positions

of the primary and secondary satellites is minimized. CARA generally calculates and employs such "at-TCA" 2D-P_c estimates for initial conjunction risk assessments. However, 2D-P_c estimates can also be calculated using states and covariances defined at times offset from TCA. If the offset time is sufficiently short (e.g., $<< \Delta t$) , such "offset-from-TCA" 2D-P_c estimates will not differ appreciably from the at-TCA estimate.[3] In fact, for most events analyzed by CARA, the offset time can span the entire short-term encounter validity interval and still yield approximately the same 2D-P_c value (as will be demonstrated later). Some conjunctions, however, show large offset-from-TCA 2D-P_c variations over their short-term encounter validity intervals.

The CARA system receives data similar to that contained in a standard *conjunction data messag*e (CDM) for each processed conjunction.[4,8] In addition to a conjunction's nominal TCA, CDMs also contain data for both the primary and secondary satellites that can be converted into at-TCA inertial-frame cartesian orbital states and associated covariance matrices.[8] Offset-from-TCA states and covariances can be estimated by propagating these at-TCA quantities both forward and backward in time over the short-term encounter validity interval, $-\Delta t \leq t \leq \Delta t$, where t indicates the offset time measured relative to nominal TCA. This analysis employs Keplerian 2-body equations of motion and transition matrices for these state/covariance propagations, which approximate the effects of both curvilinear trajectories and temporally changing covariances. These 2-body propagations can be performed directly using a cartesian position/velocity orbital state representation[9] or by converting to an equinoctial element state representation[10,11] — two approaches found to produce equivalent results in this analysis. These propagated states and covariances can then be used to calculate offset-from-TCA 2D-P_c estimates, denoted in this analysis as $P_c(t)$, with $P_{c,0} = P_c(0)$ representing the at-TCA 2D-P_c estimate.

When calculating $P_c(t)$, care must be taken to estimate offset-from-TCA close approach distances, $r_{ca}(t)$, which can differ from the at-TCA value. Significant variations in $r_{ca}(t)$ can occur if the relative primary-to-secondary trajectory curves significantly during the $-\Delta t \leq t \leq \Delta t$ interval, potentially leading to large variations in $P_c(t)$, as discussed in detail by Chan[3] (specifically, see Figure 3.3 in reference 3). This implies that large $P_c(t)$ variations can indicate that a conjunction potentially fails to satisfy the 2D-P_c assumption of linear trajectories. Similarly, variations in $P_c(t)$ can also occur if the relative position covariance matrix changes significantly during $-\Delta t \leq t \leq \Delta t$. So large $P_c(t)$ variations can also indicate a failure to satisfy the 2D-P_c assumption of constant covariance.

Figure 1 shows offset-from-TCA 2D-P_c variations for two CARA conjunctions that have been analyzed in detail previously using BFMC simulations.[4] The left plot shows the relatively small $P_c(t)$ variations calculated for a conjunction between NASA's *Aqua* satellite and a debris object, for which the 2D-P_c and BFMC-P_c method estimates match one another to within Monte Carlo estimation uncertainty (i.e., $P_{c,0} \approx$ BFMC-P_c as shown in Figure 1 of Hall *et al.*[4]). This contrasts with the right plot, which shows the large-amplitude $P_c(t)$ variations calculated for a *Van Allen* satellite conjunction, for which $P_{c,0}$ underestimates BFMC-P_c by a factor of about 300 (as shown in Figure 4 of Hall *et al.*[4]) Notably, all conjunctions found so far for which $P_{c,0}$ significantly underestimates BFMC-P_c show such large-amplitude $P_c(t)$ variations, without exception. Conversely, most conjunctions for which $P_{c,0}$ accurately matches BFMC-P_c, show relatively small $P_c(t)$ variations. As explained in more detail later, this observation provides the basis for a diagnostic test to check for potential 2D-P_c method inaccuracies.

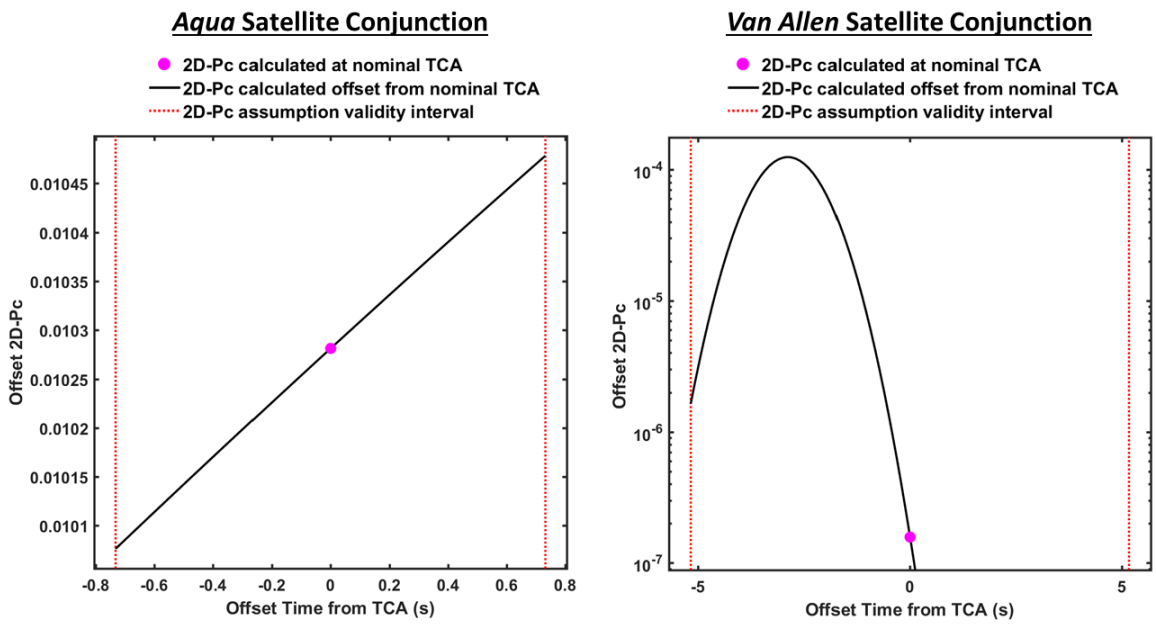

Figure 1. Offset-from-TCA 2D-P_c estimates for an *Aqua* conjunction (left) for which the 2D-P_c and BFMC-P_c estimates agree, and a *Van Allen* conjunction for which 2D-P_c significantly underestimates BFMC-P_c.

COMPARISONS OF 2D-P_c AND BFMC-P_c ESTIMATES

Figure 2 shows a comparison of at-TCA 2D-P_c estimates (horizontal axis) and BFMC-P_c estimates (vertical axis) for a representative set of 43,595 conjunctions processed by CARA from 2017-05-01 to 2018-11-15. This set includes all events archived in CARA's database over that period that have $P_{c,0} \geq 10^{-7}$ (the criterion corresponding to medium- and high-priority risk assessments performed within the CARA system), as well as a primary OD epoch age of ≤10 days and a secondary OD epoch age of ≤20 days. Conjunction short-term validity intervals vary significantly among these events, with a median Δt of 1.2 s, and a 95% range of 0.17 s ≤ Δt ≤ 9.8 s.

The BFMC-P_c estimates and error bars plotted in Figure 2 employ the "BFMC from-TCA/CDM-mode" estimation methodology described in detail in Hall *et al*.[4] (The vertical error bars represent 95% confidence BFMC-P_c uncertainty intervals.) Figure 2 indicates that major BFMC-P_c vs 2D-P_c differences occur in both directions, BFMC-P_c << $P_{c,0}$ and BFMC-P_c >> $P_{c,0}$, with the latter type causing more concern because, for these conjunctions, the 2D-P_c approximation significantly underestimates the actual conjunction risk indicated by the high-fidelity BFMC simulation, whereas the former represents an overly conservative collision risk estimation.

Large-Amplitude 2D-P_c Underestimation Inaccuracies

This analysis focuses on designing a test to detect "large-amplitude 2D-P_c underestimations" defined here as conjunctions with BFMC-$P_c/P_{c,0} \geq F_b$, where F_b denotes the factor bounding what is considered a large-amplitude underestimation. The colored diamonds in Figure 2 indicate the existence of 22 large-amplitude 2D-P_c underestimations for $F_b = 2.5$; these all appear well above the diagonal line in the plot. The black cross (+) symbols in Figure 2 show the much larger number of remaining conjunctions, plotted with error bars corresponding to 95% confidence Monte Carlo uncertainty intervals.[4] The black symbols also indicate the existence of several large-amplitude 2D-

P_c overestimations, which appear well below the diagonal line (note: several of these had zero collisions registered in the BFMC simulations, and are represented in Figure 2 using downward pointing triangles with a single-sided error bar).

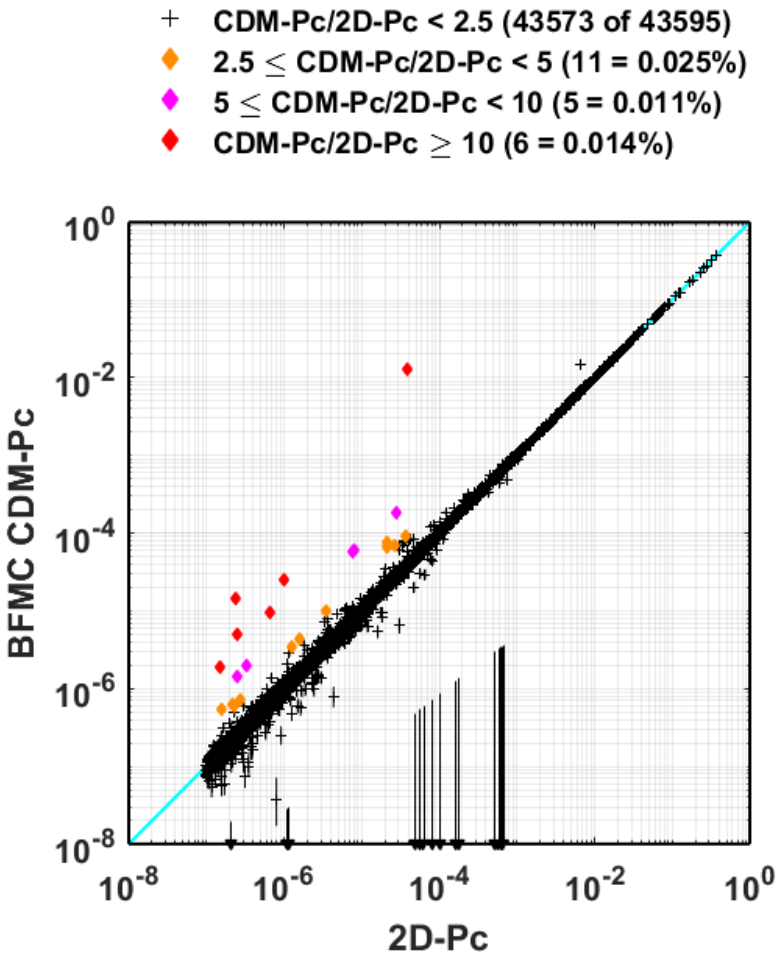

Figure 2. A comparison of 2D-P_c and BFMC-P_c estimates for 43,595 CARA conjunctions. Colored diamonds show large-amplitude 2D-P_c method underestimation inaccuracies.

The comparison shown in Figure 2 confirms that the 2D-P_c approximation produces sufficiently accurate estimates to enable effective risk assessments for the majority of CARA conjunctions.[4] Among this representative set of ~44,000 conjunctions, only 22 events suffer from 2D-P_c underestimations by a factor of $F_b = 2.5$ or more; 11 of these represent underestimations for $F_b = 5$, and 6 for $F_b = 10$. Assuming that the data set analyzed here is representative of future conjunctions, these small fractions can be interpreted as probabilities that such 2D-P_c underestimations will occur in the future, equaling ~5×10^{-4}, ~2.5×10^{-4}, and ~1.4×10^{-4}, respectively, for the F_b values given above. Notably, these probabilities exceed (but are roughly comparable to) the "red" collision probability of 10^{-4} that the CARA team employs for high-priority risk assessments, which can ultimately lead to satellite operators planning and executing maneuvers to mitigate collision risk. This probability comparison emphasizes the need for a procedure to detect and mitigate 2D-P_c underestimation inaccuracies.

Measuring Offset-from-TCA 2D-P_c Variations

As discussed previously, large variations in offset-from-TCA 2D-P_c estimates can indicate that a conjunction potentially fails to satisfy the 2D-P_c assumptions of linear motion and/or constant relative position covariance. Measuring the amplitude of such $P_c(t)$ variations forms the basis of the 2D-P_c method diagnostic test and usage boundaries presented in this analysis. One measure of the amplitude of $P_c(t)$ variations can be defined as

$$V' = \log_{10}\left[P_c^{min}/P_c^{max}\right] \tag{2}$$

where

$$P_c^{min} = \min_{|t|\leq\Delta t}\left[P_c(t)\right] \qquad \text{and} \qquad P_c^{max} = \max_{|t|\leq\Delta t}\left[P_c(t)\right] \tag{3}$$

denote the extrema over the short-term encounter validity interval, $-\Delta t \leq t \leq \Delta t$. These extrema can be determined numerically (e.g., using a bisection search optimization method[12]). Analysis indicates that the metric V' can be used as an indicator of overall 2D-P_c method inaccuracies, including both underestimations and overestimations. A slightly different variation metric, however, has been found to perform somewhat better as a diagnostic indicator of potential 2D-P_c underestimations alone, in that it produces fewer false alarms

$$V = \log_{10}\left[P_c^{min}/P_c^{mid}\right] \tag{4}$$

where

$$P_c^{mid} = (P_{c,0} + P_c^{min})/2 \tag{5}$$

denotes the midpoint between the at-TCA and minimum offset-from-TCA 2D-P_c values. For reference, the *Aqua* satellite conjunction with the small $P_c(t)$ variations shown on the left panel of Figure 1 has $V = 0.013$ measured over an interval with half-width Δt = 0.7 s, whereas the *Van Allen* event shown on the right panel has a much larger variation of $V = 3.2$ over Δt = 5 s.

Notably, calculating V requires numerically finding the minima and maxima of $P_c(t)$ over the validity interval $-\Delta t \leq t \leq \Delta t$, which entails many 2D-$P_c$ method computations. This increased computational load can be reduced by using a software implementation of the 2D-P_c method optimized for computation speed.

Including the Effects of Non-Positive Definite Covariances

The metric V can be modified to additionally include the effects of inaccuracies introduced by NPD state covariance matrices. As discussed previously, NPD covariances indicate a potential violation of the first of the three 2D-P_c method assumptions. NPD covariances also represent physically implausible uncertainty distributions, and can potentially prevent P_c estimation.[8] For instance, the 2D-P_c method employs a marginalized 2×2 covariance matrix indicating the combined relative position uncertainty projected onto the conjunction plane[1-3,5], and cannot provide a physically-plausible estimate if this 2×2 matrix is NPD.[8] Fortunately, this occurs with a near-zero frequency for CARA conjunctions (e.g., in about 1 out of 800,000 events[8]). No at-TCA 2×2 marginalized covariances were found to be NPD among the ~44,000 conjunctions analyzed here.

This analysis seeks to identify differences between the 2D-P_c method and BFMC simulations. BFMC's CDM-mode samples at-TCA equinoctial element state distributions for the primary and secondary satellites, and propagates the sampled states to determine how frequently collisions occur.[4] Unfortunately, this Monte Carlo sampling process cannot employ NPD equinoctial state 6x6 covariances, which occur with non-zero frequency in CARA processing.[8] During BFMC CDM-mode processing, if one or both of the at-TCA primary or secondary equinoctial state covariances

is found to be NPD, they are remediated using an eigenvalue clipping method.[4,8] To check if this affects the 2D-P_c vs BFMC-P_c comparison, these remediated equinoctial state covariances can be converted to cartesian state covariances, and then used as an alternate inputs for the 2D-P_c method. Specifically, in such cases, this analysis generates two $P_c(t)$ curves for the unremediated and remediated covariances, and modifies the extrema from eq. (3) to include variations from both as follows

$$P_c^{min} = \min\{\min_{|t|\leq\Delta t}[P_c^u(t)], \min_{|t|\leq\Delta t}[P_c^r(t)]\} \text{ and } P_c^{max} = \max\{\max_{|t|\leq\Delta t}[P_c^u(t)], \max_{|t|\leq\Delta t}[P_c^r(t)]\} \quad (6)$$

where $P_c^u(t)$ represents offset-from-TCA 2D-P_c estimates for the unremediated covariances, and $P_c^r(t)$ for the remediated covariances. With these modifications, a variation metric V that includes NPD effects can be calculated using eqs. (4) and (5). The $P_{c,0}$ value used in eq. (5) for this analysis, however, still represents the at-TCA 2D-P_c estimated with the raw, unremediated conjunction covariance matrices.

Using Offset-from-TCA 2D-P_c Variations as an Indicator of Underestimation Inaccuracies

Figure 3 shows the distribution of BFMC-P_c/2D-P_c ratios as a function of the offset-from-TCA variation metric calculated as described above for the representative set of conjunctions analyzed here. Specifically, the top panel shows how BFMC-$P_c/P_{c,0}$ ratios (vertical axis) vary with V (horizontal axis). Again, the 22 colored diamonds show 2D-P_c underestimations exceeding a factor of $F_b = 2.5$ (with the same color coding used in Figure 2), and the black cross (+) symbols show the remaining events (plotted with no error bars here for clarity). The bottom panel of Figure 3 shows cumulative distribution functions (CDFs) for these sets (also using the same color coding).

The CDF curve plotted in black in Figure 3 indicates that most of the analyzed conjunctions have relatively small variation metrics: about half (53.5%) have $V \leq 0.1$ and two thirds (66.3%) have $V \leq 0.2$. However, all 22 conjunctions with 2D-P_c underestimation factors exceeding $F_b = 2.5$ show variation metrics with $V > 0.8$. Notably, about 9% (or ~3,900) of the remaining events also have variation metrics above this boundary value of $V_b = 0.8$. This means that the variation metric V does not provide a perfect means of predicting such large-amplitude 2D-P_c underestimations, but can be used as an indicator of potential underestimations. Assuming that the analyzed conjunction data set is representative of future events, this study indicates that if a future conjunction is found to have a variation metric exceeding a boundary value of $V_b = 0.8$, then the 2D-P_c method could potentially underestimate the actual P_c by a factor of $F_b = 2.5$ or more. To know definitively, a BFMC-fidelity method can then be used to estimate the actual P_c, which usually comes at the cost of considerably increased computation.

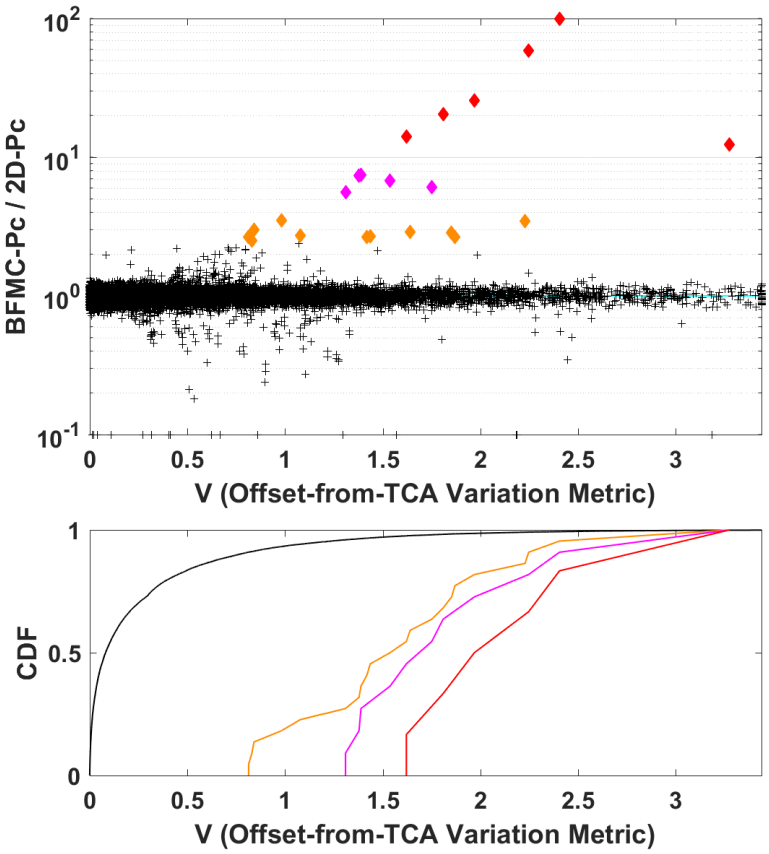

Figure 3. The distribution of BFMC-P_c/2D-P_c ratios plotted as a function of the variation metric V (top panel) with corresponding CDFs (bottom panel). Colored diamonds show 2D-P_c method underestimations that exceed a factor of 2.5, which occur only for $V > 0.8$.

A Diagnostic Test to Detect Potential 2D-P_c Underestimation Inaccuracies

The test procedure developed in this study to diagnose potential 2D-P_c method underestimations and mitigate associated risks can be summarized as follows: if the variation metric for an individual conjunction exceeds a boundary value (i.e., $V > V_b$), then the 2D-P_c method might underestimate the actual collision probability by a factor of F_b or more, and a high-fidelity P_c estimate should be computed. The effectiveness of this diagnostic test can be characterized by how frequently it produces false alarms and missed detections. False alarms occur for conjunctions with $V > V_b$ for which the 2D-P_c method does not underestimate the actual collision probability by a factor of F_b or more. Missed detections occur for conjunctions with $V \leq V_b$ for which 2D-P_c does underestimate the actual probability by a factor of F_b or more. Missed detections represent the more serious type of diagnostic error, because they can lead to a failure to detect and mitigate actual collision risks. False alarms, on the other hand, only prompt high-fidelity P_c computations, which may require extra time and effort to complete, but ultimately yield higher quality risk assessments.

Based on the previous discussion of Figure 3, this diagnostic test should be expected to have a high false alarm frequency, because it most often will not reveal large-amplitude 2D-P_c underestimations. Assuming that the analyzed data set is representative of future conjunctions, applying the test using a boundary metric of $V_b = 0.8$ will prompt high-fidelity P_c computations for ~9% of

future events (the fraction with $V > V_b$) in order to find the ~0.05% of future events that suffer from actual 2D-P_c underestimations with amplitude $F_b = 2.5$ or greater.

The test's frequency of missed detections can be reduced by adjusting the boundary value V_b. Again, assuming that the data set analyzed here is perfectly representative (or nearly representative) of future conjunctions, then the choice of $V_b = 0.8$ by design will reveal all (or most) 2D-P_c underestimations with amplitude $F_b = 2.5$ or greater, corresponding to a zero (or small) frequency of missed detections.

Estimated Usage Boundaries for the 2D-P_c Estimation Method

Table 1 reports the number of missed detections in the analyzed data set as a function of V_b and F_b, formatted to ease estimating usage boundaries for the 2D-P_c method and diagnostic test. Specifically, the first column of Table 1 lists the fraction of events with $V > V_b$, and the second column lists the corresponding V_b value. The remaining columns tabulate the number of events for which 2D-P_c underestimates BFMC-P_c by a factor of F_b or more, for F_b values of {2.0, 2.5, 3.0, 5.0, 10.0}. The green/yellow/red color shading indicates the frequency of missed detections. Specifically, green indicates no missed detections, yellow a missed detection frequency of $\leq 10^{-4}$, and red a missed detection frequency $>10^{-4}$. Table 1 can be used to estimate diagnostic test usage boundaries given a desired bounding underestimation factor F_b. For instance, eliminating all missed detections for a 2D-P_c underestimation factor of $F_b = 10$, requires a boundary of $V_b \approx 1.49$, prompting high-fidelity P_c computations for about 3% of all events. Similarly, eliminating all missed detections at a level of $F_b = 2$, requires $V_b \approx 0.14$ and high-fidelity computations for about 40% of all events.

Table 1. Missed detections as a function of V_b and F_b. Green shading indicates no missed detections, yellow a missed-detection frequency of $\leq 10^{-4}$ and red a frequency of $>10^{-4}$.

Fraction with $V \geq V_b$ (%)	Variation Metric Boundary, V_b	2D-P_c Underestimation Boundary Factor, F_b				
		2.0	2.5	3.0	5.0	10.0
0.0	∞	34	22	14	11	6
1.0	2.19	30	18	10	8	3
2.0	1.75	26	14	8	6	1
3.0	1.49	22	10	5	3	0
5.0	1.18	16	5	2	0	0
7.5	0.93	13	3	1	0	0
10.0	0.76	7	0	0	0	0
12.5	0.64	2	0	0	0	0
15.0	0.54	2	0	0	0	0
20.0	0.41	1	0	0	0	0
30.0	0.25	1	0	0	0	0
40.0	0.14	0	0	0	0	0

DISCUSSION

This analysis demonstrates that the 2D-P_c method occasionally underestimates actual conjunction collision probabilities, and that offset-from-TCA variations can be used as a diagnostic indicator of such inaccuracies. During the research and development of the specific test presented here, the CARA analysis team investigated several other candidate diagnostic indicators, with varying degrees of success. These include indicators based on a conjunction's short-term encounter validity

interval itself, Δt, as well as its ratio to the minimum primary/secondary orbital period. Another set of candidates measured Mahalanobis distance variations caused by including or excluding various effects to test a conjunction's adherence to the 2D-P_c assumptions, such as linear vs curved trajectories, zero vs non-zero velocity uncertainties, and remediated vs unremediated NPD covariances. Finally, another candidate indicator measured P_c differences between the 2D-P_c method and a different semi-analytical P_c estimation method.[13] None of these candidate indicators were found to work as well as the one presented here, based on their observed frequencies of raising false alarms and, more importantly, of failing to detect large-amplitude 2D-P_c underestimations.

CONCLUSIONS

The analysis yields the following conclusions:

1. The 2D-P_c method underestimates high-fidelity BFMC CDM-mode P_c values by a factor of 2.5 or more for a small fraction (~0.05%) of the 43,595 representative CARA conjunctions analyzed in this study.
2. In order to provide an accurate estimate for a conjunction, the 2D-P_c method depends on three assumptions being satisfied: 1) the relative primary-to-secondary position uncertainty distribution can be approximated using a single 3×3 covariance matrix; 2) the relative satellite trajectories can be approximated as rectilinear; and 3) the relative position covariance matrix can be approximated as constant. Ideally, these 2D-P_c assumptions should be satisfied during a conjunction-specific time period known as the *short-term encounter validity interval*, TCA ± Δt.[5]
3. Offset-from-TCA 2D-P_c estimates, $P_c(t)$, can be approximated throughout a conjunction's short-term encounter validity interval by using 2-body state/covariance propagation, initiated with at-TCA states and covariances (such as those contained in a CDM).
4. Large-amplitude $P_c(t)$ variations indicate potential violations of the 2D-P_c assumptions, and can be quantified using the offset-from-TCA variation metric, V.
5. All conjunctions found to date for which 2D-P_c significantly underestimates BFMC-P_c have relatively large V metrics. Most conjunctions for which 2D-P_c accurately matches BFMC-P_c, have relatively small V metrics.
6. The 2D-P_c underestimation diagnostic test procedure can be summarized as follows: if the variation metric for a conjunction exceeds a specified boundary value (i.e., $V > V_b$), then the 2D-P_c method might underestimate the actual collision probability by a corresponding factor of F_b or more, and a high-fidelity P_c estimate should be computed.
7. The diagnostic test has a high false alarm rate because it prompts a relatively large number of high-fidelity P_c computations, in order to find a much smaller number of actual large-amplitude 2D-P_c method underestimations.
8. The missed detection rate for the diagnostic test can be reduced by adjusting the boundary metric value, V_b. Among the data analyzed in this study, a value of $V_b = 0.8$ eliminates all missed detections when testing for 2D-P_c underestimations of amplitude $F_b = 2.5$ or greater. Table 1 reports the frequency of missed detections for other boundary values of V_b and F_b.

SYMBOLS AND ACRONYMS

F_b = the factor bounding what is considered a large-amplitude 2D-P_c underestimation
P_c = probability of collision for a conjunction between a primary and secondary satellite
$P_c(t)$ = a 2D-P_c value estimated using states and covariances for an offset-from-TCA time t
$P_c^r(t)$ = a $P_c(t)$ curve calculated using remediated at-TCA postion+velocity covariances
$P_c^u(t)$ = a $P_c(t)$ curve calculated using unremediated at-TCA postion+velocity covariances
$P_{c,0}$ = $P_c(0)$ = the at-TCA 2D-P_c estimate (i.e., estimated at a zero offset-from-TCA time)

P_c^{min} = the minimum $P_c(t)$ over the short-term encounter validity interval $-\Delta t \leq t \leq \Delta t$
P_c^{mid} = the mid-point value between $P_{c,0}$ and P_c^{min}
P_c^{max} = the maximum $P_c(t)$ over the short-term encounter validity interval $-\Delta t \leq t \leq \Delta t$
$r_{ca}(t)$ = the close-approach distance estimated for an offset-from-TCA time t
t = an offset time measured relative to a conjunction's nominal TCA
V = the offset-from-TCA 2D-P_c variation metric, measuring the amplitude of $P_c(t)$ variations
V_b = a boundary V value; $V \geq V_b$ indicates potential large-amplitude 2D-P_c underestimations
V' = an alternate metric measuring the amplitude of $P_c(t)$ variations

Δt = the half-width of a conjunction's short-term encounter validity interval
γ = the precision tolerance used to define a conjunction's duration, taken to be 10-16 here
τ_0 = the begin-time of a conjunction's encounter duration measured relative to TCA
τ_1 = the end-time of a conjunction's encounter duration measured relative to TCA

2D = two-dimensional
2D-P_c = a collision probability estimated using the 2D collision probability method
BFMC = brute force Monte Carlo
BFMC-P_c = a collision probability estimated using a BFMC simulation
CARA = Conjunction Assessment Risk Analysis
CDM = conjunction data message
NPD = non-positive definite
OD = orbit determination
NASA = National Aeronautics and Space Administration
TCA = time of closest approach

ACKNOWLEDGMENTS

The author would like to thank Luis Baars, Steve Casali, Joseph Frisbee, Matthew Hejduk, Travis Lechtenberg, and Daniel Snow for several helpful discussions and analyses. The CARA analysis team would like to thank Salvatore Alfano for suggesting the amplitude of offset-from-TCA P_c variations as an indicator of potential 2D-P_c method inaccuracies.

REFERENCES

[1] J.L. Foster and H.S. Estes, "A Parametric Analysis of Orbital Debris Collision Probability and Maneuver Rate for Space Vehicles," NASA/JSC-25898, Aug. 1992.
[2] M.R. Akella and K.T. Alfriend, "The Probability of Collision Between Space Objects," *Journal of Guidance, Control, and Dynamics*, Vol. 23, No. 5, pp. 769-772, 2000.
[3] K. Chan, *Spacecraft Collision Probability*, El Segundo, CA, The AeroSpace Corporation, 2008.
[4] D. Hall, S.J. Casali, L.C. Johnson, B.B. Skrehart, and L.G. Baars, "High-fidelity Collision Probabilities Estimated Using Brute Force Monte Carlo Simulations," *AAS Astrodynamics Specialist Conference*, Snowbird, UT, Paper 18-244, Aug. 2018.
[5] V.T. Coppola, "Evaluating the Short Encounter Assumption of the Probability of Collision Formula," *AAS/AIAA Spaceflight Mechanics Meeting*, Charleston SC, Paper 12-248, Feb. 2012.
[6] B.D. Tapley, B.E. Schutz, and G.H. Born, *Statistical Orbit Determination*, Elsevier Academic Press, Burlington, MA, 2004.
[7] D.A. Vallado, *Fundamentals of Astrodynamics and Applications*, 2rd ed., Microcosm Press, El Segundo CA, 2001.

[8] D.T. Hall, M.D. Hejduk, and L.C. Johnson, "Remediating Non-Positive Definite State Covariances for Collision Probability Estimation," *AAS Astrodynamics Specialist Conference*, Columbia Valley, WA, Paper 17-567, 2017.
[9] S.W. Shepperd, "Universal Keplerian State Transition Matrix," *Celestial Mechanics*, Vol. 35, pp. 129-144, 1985.
[10] D. Vallado, "Covariance Transformation for Satellite Flight Dynamics Operations," *AAS/AIAA Astrodynamics Specialist Conference*, Big Sky, MT, Paper 03-526, 2003.
[11] D. Vallado and S. Alfano, "Updated Analytical Partials for Covariance Transformations and Optimization," *AAS/AIAA Space Flight Mechanics Meeting*, Williamsburg, VA, Paper 15-537, 2015.
[12] W.H. Press *et al*, *Numerical Recipes in FORTRAN: The Art of Scientific Computing*, 2nd edition, Cambridge University Press, New York, NY, 1992.
[13] V.T. Coppola, "Including Velocity Uncertainty in the Probability of Collision between Space Objects," *AAS/AIAA Spaceflight Mechanics Meeting*, Charleston SC, Paper 12-247, Feb. 2012.